Poly(vinyl acetate)/Silica Filled Materials: Material Properties of in Situ vs Fumed Silica Particles

Christine J. T. Landry,* Bradley K. Coltrain, and Michael R. Landry

Corporate Research Laboratories, Eastman Kodak Company, Rochester, New York 14650-2116

John J. Fitzgerald

Imaging Research Laboratories, Eastman Kodak Company, Rochester, New York 14650-2135

Victoria K. Long

Analytical Technology Division, Research Laboratories, Eastman Kodak Company, Rochester, New York 14650-2110

Received November 23, 1992

ABSTRACT: Composites of poly(vinyl acetate) (PVAc) and silica were prepared from the in situ polymerization of acid-catalyzed tetraethoxysilane. The physical properties of these composites were compared with those of PVAc/fumed silica (of 7-nm nominal particle size) composites prepared by both melt-milling and solution-casting from tetrahydrofuran or carbon tetrachloride. Their morphologies were examined by transmission electron microscopy and small-angle X-ray scattering revealing that, although all the materials were optically transparent, differences in the primary particle size and interfacial regions exist. Infrared spectroscopy showed that substantially more hydrogen bonding occurs in the in situ prepared composites. The dielectric, dynamic mechanical, and ultimate mechanical properties of the composites indicated that a connected, supporting silicate network phase is formed at much lower concentrations of silica in the in situ prepared composites. This is shown to have a substantial effect on the tensile properties of the composite at temperatures above the glass transition temperature (T_g) of PVAc but does not dramatically influence these properties below T_g.

Introduction

Composite materials consisting of organic polymers and inorganic oxide particles or fibers are utilized in numerous applications. Often the filler particle or fiber is surface treated with silane coupling agents to aid dispersion in a polymeric resin and to improve adhesion between the phases.[1,2] Silane coupling agents generally are organofunctional silanes of the type R_nSiX_{4-n}, where R is a nonhydrolyzable organic radical such as phenyl or aminopropyl and X is a hydrolyzable group such as halide or alkoxide. The dimensions of the fiber or particle, as well as the amount of particle aggregation, define the inorganic domain size in these types of composites.

Recently, numerous reports have appeared on the preparation of organic–inorganic composites (OICs) by in situ polymerization of metal alkoxides (or related monomers) in organic polymers.[3-28] The nature and structure of the inorganic oxide generated by hydrolysis and condensation of metal alkoxides can be controlled with such variables as pH, the amount of water added for hydrolysis, and the type of solvent employed.[29] The fact that this chemistry can proceed at low temperatures makes it amenable to combining with organic polymers.

The degree of homogeneity or phase separation between the organic and inorganic components can be controlled using this in situ method. One approach utilizes organic polymers functionalized with trialkoxysilane moieties to facilitate cross-linking between the polymer and the growing inorganic oxide network.[3-13] Cross-reaction of the organic and inorganic components retards phase separation, frequently producing homogeneous hybrid materials. Alternatively, it is possible to produce homogeneous, transparent OICs with highly dispersed inorganic oxide phases using organic polymers *without* trialkoxysilane functionality if appropriate polymer backbones are used.[14-25] This approach relies upon specific interactions, such as hydrogen bonding, between the organic and inorganic components to retard phase separation. For example, it has been shown that transparent composites can be obtained by the acid-catalyzed polymerization of tetraethoxysilane (TEOS) in the presence of poly(vinyl acetate) (PVAc),[16] poly(methyl methacrylate) (PMMA),[17,18] and poly[bis(methoxyethoxyethoxy)phosphazene] (MEEP).[19,20] In the cases of PVAc and PMMA, extensive hydrogen bonding was found to exist between the silanols of the silicate network and the carbonyl groups on the polymer. The strong interaction between the polymers and the silicate network apparently retards phase separation and homogenizes the two components.

One additional approach involves simultaneous polymerization of inorganic and organic monomers. Novak and co-workers have optimized reaction conditions producing highly homogeneous composites by using ring-opening metathesis polymerization (ROMP) of cyclic alkenyl monomers simultaneously with fluoride-catalyzed polymerization of tetramethoxysilane.[26-28]

It is of interest to determine how the properties of in situ generated OICs compare with those of traditional particle-filled composites. Direct comparisons are difficult since most conventional composites utilize filler particles that are frequently 0.5 μm or larger in diameter. Hydrolysis and condensation of silicon alkoxides under acid catalysis conditions leads to ramified structures, that is, mass fractals with fractal dimensions between 2 and 3.[29] However, the ramified networks can be thought of as arising from polymerization of primary particles of approximately 1 nm in size.[30] Thus, the relative sizes and surface areas of the "fillers" are quite different.

Another consideration is whether to compare properties of composites made with surface-treated particles. As described earlier, surface treatment with silane coupling

0024-9297/93/2226-3702$04.00/0

Table I. Samples

sample	wt % SiO_2 nominal	NA[a]	TGA[b]
PVAc/TS-720 (milled)	5	5.1	5.3
	20	20.5	18.2
PVAc/TS-720 (THF)	30	29.7	30.7
PVAc/MS-7 (milled)	5	5.1	4.4
	20	19.5	18.4
PVAc/EH-5 (milled)	20	17.8	17.3
	30	25.9	27.1
PVAc/EH-5 (THF)	20	22.2	23.9
	20	19.5	20.9
	30	34.9	35.1
	30	31.4	31.5
PVAc/EH-5 (CCl_4)	20	28.7	22.6
PVAc/EH-5 (THF/EtOH)	20	26.1	22.3
PVAc/TEOS	5	6.8	
	10	11.8	
	15	16.7	16.1
	20	21.0	
	30	28.2	

[a] Neutron activation results for Si. The weight percent SiO_2 was calculated assuming full condensation of the TEOS. [b] Weight percent residue above 900 °C in air.

agents greatly influences composite properties. Although the in situ composites can be generated with organic functionalities mimicking silane surface treatments, this is generally not done. Finally, filler particles are available with a variety of compositions. These can be, for example, silica, titania, or mixed metal oxide particles. The particle surface composition also affects polymer–filler interactions.

One previous study reported results comparing mechanical properties of composites of triethoxysilane-endcapped poly(dimethylsiloxane) filled with trimethylsilyl-treated silica to those of in situ polymerized TEOS.[6] The samples with commercial silica were shown to have inferior ultimate properties, particularly lower rupture energy and elongation. However, this study compared only surface-treated particles with in situ polymerized TEOS.

The present paper describes a comparison of spectroscopic, thermal, dielectric, mechanical, and morphological properties of silicate composites with PVAc generated by in situ polymerization of TEOS or by melt and/or solution blending with fumed silica. The fumed silica aggregates consisted of small (~7 nm) primary particles and were chosen for the comparison, as these are the closest in size of any of the commercially available silica fillers to that of the primary particles generated by hydrolysis and condensation of TEOS under acid conditions. Fillers composed of pure silica and silica treated with poly(dimethylsiloxane) were studied.

Experimental Section

Poly(vinyl acetate) used for the melt-milled samples was purchased from Scientific Polymer Products and was purified by precipitation into hexane. The absolute number-average ($\bar{M}_n$) and weight-average ($\bar{M}_w$) molecular weights, determined by size exclusion chromatography (SEC), are 64 000 and 193 000, respectively. The PVAc used for all other samples was purchased from Polysciences and has $\bar{M}_n$ = 57 000 and $\bar{M}_w$ = 220 000, as determined by SEC. TEOS was purchased from Fluka and was used without further purification. Cab-O-Sil TS-720 is a fumed silica that has been treated with a dimethylsilicone fluid and has a reported nominal particle size of 14 nm. Cab-O-Sil MS-7 and EH-5 are amorphous fumed silica with reported nominal particle sizes of 14 and 7 nm, respectively. All Cab-O-Sil samples were purchased from Cabot Corp.

A listing of the composites can be found in Table I. The preparation of the in situ composites has been reported previously[16] and consists of the addition (under continuous mixing) of TEOS to a 20 wt % solution of PVAc in THF, followed by the addition of a stoichiometric amount of water (based on the number of alkoxide substituents) in the form of 0.15 M HCl. The solutions were mixed at ambient temperature for 65 h, knife-coated, dried, and finally cured under vacuum for 20 h at 100 °C or as indicated in the text. All films were optically transparent. Alternatively, a few samples were prepared by the addition of prehydrolyzed TEOS (where a stoichiometric amount of 0.15 M HCl was added to a 1/1 mixture of TEOS and THF and the mixture was allowed to react for 5 days) to the PVAc/THF solution, immediately followed by coating and drying.

The Cab-O-Sil filled composites were prepared by two different methods. The first involved adding the Cab-O-Sil to molten PVAc in a two-roll mill and mixing at ca. 100 °C for 20 min. The mixture was then melt-pressed at 100–120 °C to obtain thin, optically transparent films. Some shear degradation of the PVAc molecular weight occurred during the milling process; however, $\bar{M}_w$ did not drop below 140 000 and $\bar{M}_n$ showed a slight increase. In the second method, the Cab-O-Sil was added to a 10 wt % solution of PVAc in THF and mixed for several hours. The solution was then cast into a Teflon mold, covered, and dried. This produced opaque, broken pieces of the composites. Transparent thin films of these could then be obtained by melt-pressing at 100–120 °C. Samples were produced in other solvents (CCl_4 or a THF/EtOH mixture) in an analogous manner. Using either method, the highest loading of Cab-O-Sil EH-5 that could be melt-processed was between 28 and 35 wt %. In the first method the limiting factor was abrasion of the brass shanks on the side of the mill, and in the second, the ability of the sample to flow and consolidate in the press at temperatures low enough to avoid color formation in the sample (below 150 °C). The samples were dried at 100 °C for 20 h under vacuum and further cured as indicated in the text. All samples were stored under vacuum or nitrogen prior to use, since they are hygroscopic. The absorption of moisture is easily detected by a depression in T_g.

The final SiO_2 contents of the samples (Table I) were determined by neutron activation (NA) (silicon analysis) and by thermal gravimetric analysis (TGA) (weight percent residue above 900 °C in air) and are listed in Table I. For the in situ prepared composites the weight percent SiO_2 was calculated from the measured Si content, assuming full condensation of the silicate. In the discussion of the results, the samples are generally referred to by the nominal weight percent SiO_2.

The dynamic mechanical (DMA) properties of the composites were measured using a Rheometrics solid analyzer (RSA-II). The driving frequency was 10 Hz and the temperature was typically scanned between −100 and +300 °C at a rate of 2–3 °C/min. Some of the melt-pressed PVAc/EH-5 samples, as prepared, had large cross-sectional areas and taxed the limits of the RSA-II (instrument compliance). Thus, the E' values in the glassy regime obtained by DMA should not be viewed as quantitative.

Dielectric properties (DE) were measured with a Hewlett-Packard Model 4192a impedance analyzer interfaced with a Gateway 386 PC. At each temperature, 20 frequencies were measured between 10^2 and 10^6 Hz. The temperature was controlled with an environmental chamber (Delta Design oven 9023). Samples for DE measurement were generally about 100 μm thick.

Mechanical properties were measured on a Sintech 20 testing machine. Miniature dogbone samples, ASTM D638m-III format, were tested at a constant crosshead speed of 2.5 mm/min (strain rate = 0.1 min^{-1}). The engineering stress was calculated using the average cross-sectional area. The strain was calculated using the crosshead displacement and an effective gage length. The tensile modulus was determined using a linear regression fit of the initial slope of the stress–strain curve.

Fourier transform infrared (FTIR) spectra of the films were obtained in the reflectance mode (ATR) (germanium crystal) using a Bio-Rad (Digilab Division) FTS-7 spectrometer (3240-SPC). Transmission spectra of PVAc/EH-5 solutions in THF and CCl_4 (between two KBr disks) were obtained using a Nicolet 20SXB FTIR spectrometer. The resolution used was 4 cm^{-1}.

Small-angle X-ray scattering (SAXS) measurements were performed on 0.2-mm-thick film specimens using an Anton Paar compact Kratky camera equipped with a Braun linear position sensitive detector. The SAXS profiles were corrected for parasitic

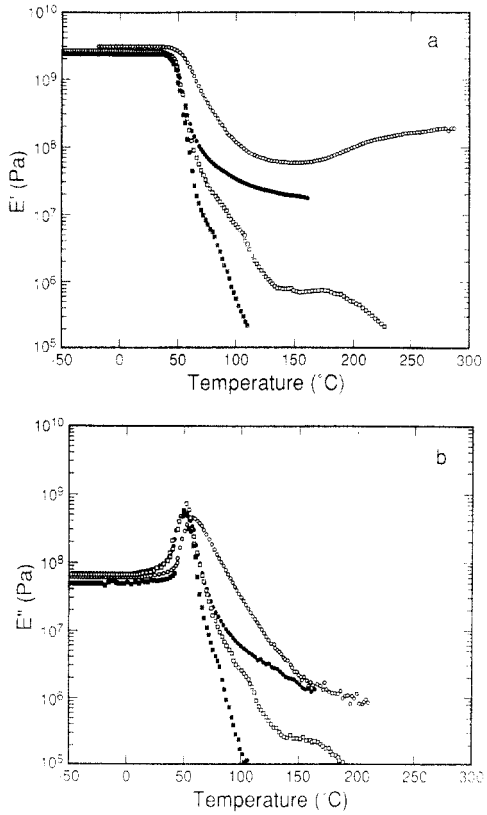

Figure 1. Temperature dependence of (a) the storage modulus and (b) the loss modulus for PVAc composites containing (○) 21 wt % SiO_2 from TEOS, (●) 23 wt % EH-5 cast from THF, (□) 20 wt % EH-5 cast from THF, and (■) 18 wt % EH-5 melt-milled.

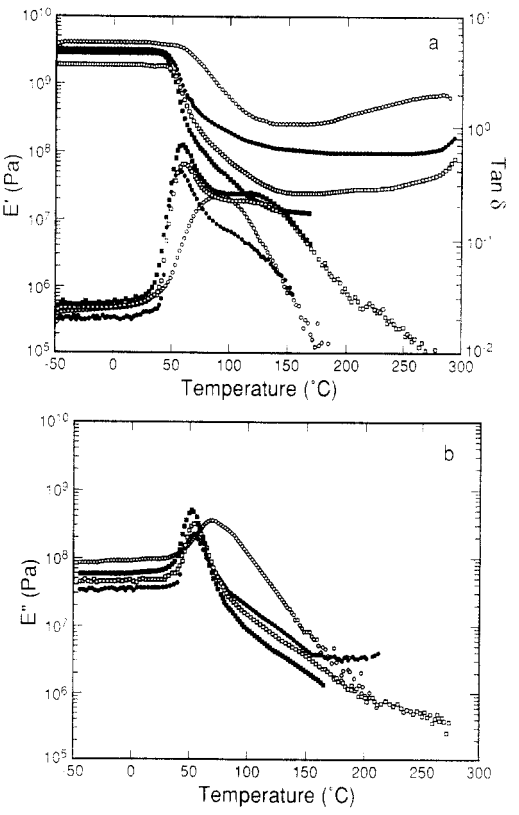

Figure 2. Temperature dependence of (a) the storage modulus and tan δ and (b) the loss modulus for PVAc composites containing (○) 28 wt % SiO_2 from TEOS, (●) 35 wt % EH-5 cast from THF, (□) 31 wt % EH-5 cast from THF, and (■) 27 wt % EH-5 melt-milled.

scattering, detector homogeneity, and the contribution of background scattering from the PVAc phase. The latter correction was done by subtracting the SAXS profile of pure PVAc, weighted by its volume fraction, which shows a gradual increase throughout the scattering vector range q of 0.001–0.05 nm^{-1}, where $q = (4\pi/\lambda)\sin(\theta/2)$, and λ and θ are the X-ray wavelength and scattering angle, respectively. The volume fractions were calculated from the measured weight fraction of the silicate phase (Table I), using a mass density for PVAc of 1.2 g cm^{-1} and 2.2 g cm^{-1} for the skeletal density of the silicate phase.[31] Implicit in the procedure for removing the background scattering is the assumption that the filler phase does not affect the amorphous structure of the polymer. All profiles were desmeared for the effects of slit collimation of the Kratky camera.[32]

Samples for transmission electron microscopy (TEM) were sectioned with a diamond knife at 23 °C, giving sections approximately 50 nm thick. TEM was performed using a Philips 400T microscope. The intrinsic contrast between the organic polymer and the SiO_2 particles was sufficient such that no staining was required.

Experimental Results

The persistence of a high tensile modulus, E', above the glass transition temperature of PVAc and a broadening of the distribution of the PVAc chain relaxation times at T_g were previously[16] observed for PVAc composites prepared via the in situ polymerization of silicon alkoxide. The interpretation was that a supporting and continuous silicate network was formed along with an interfacial region in the composites where the mobility of the PVAc chains is reduced by the interactions with, and possible entrapment within, the silicate network. Similar properties have also been reported in other composites prepared via the in situ polymerization of metal alkoxides.[17,20,22,24] The question posed here is how do the properties of these in situ composites compare with those of more conventional silica-filled polymer composites. Although the fumed silica particles were very small, chosen so that the primary particle size was as close as possible to that of the in situ prepared silicate, the silica densities are different. The specific gravity of Cab-O-Sil is 2.2 g/cm^3, whereas that of silicate xerogel prepared from the polymerization of acid-catalyzed TEOS typically falls in the range of 1.4–1.65 (bulk density) or 1.9–2.2 (skeletal density), prior to densification at high temperatures.[31,33] It is thought that a more open, ramified network structure exists in the latter systems within which polymer chains can entangle and interpenetrate.

Dynamic and Ultimate Mechanical Properties. The DMA results for composites containing 20 and 30 wt % SiO_2 are summarized in Figures 1 and 2, respectively. Parts a and b of Figure 1 compare the temperature dependence of the Young's storage (E') and loss (E'') moduli for the various composites containing approximately 20 wt % SiO_2. The DMA curves for the melt-milled PVAc/EH-5 sample are very similar to those obtained for pure PVAc. The peak in E'' (and also in tan $\delta = E''/E'$; not shown) at T_g is narrow, having a maximum at 50 °C. No rubberlike plateau in E' above T_g is observed, and the composite undergoes viscous flow above T_g. The DMA curves for composites containing 20 wt % MS-7 and TS-720 were identical to those for the melt-milled EH-5 composites. In contrast, the sample prepared from TEOS exhibits a plateau in the storage modulus above T_g that is greater than 10^8 Pa and persists to temperatures as high as ca. 300 °C. The latter sample was cured at 130 °C for 3 h under vacuum to ensure complete solvent removal and to remove any artifacts in the temperature dependence of E' due to condensation chemistry as the silicate phase undergoes further reaction (see ref 16). The peak in E'' at T_g is seen to broaden substantially, particularly on the high-tem-

Table II. Mechanical Properties of PVAc Composites at 26 °C[a]

sample	wt % SiO_2	modulus (MPa)	break stress (MPa)	break strain (%)	yield stress (MPa)	yield strain (%)
PVAc (solution-cast)	0	2746 (60)	35 (1)	5.2 (1.9)	42 (1)	1.7 (0)
PVAc/TEOS	7	2907 (74)	38 (2)	3.0 (1.0)	44 (1)	1.7 (0)
	12	3060 (62)	41 (2)	3.0 (0.9)	47 (1)	1.7 (0)
	16	3089 (213)	45 (6)	1.7 (0.3)		
	21	3225 (295)	44 (6)	1.5 (0.3)		
	28	3164 (243)	39 (5)	1.3 (0.2)		
PVAc (melt-milled)	0	2686 (157)	39 (3)	4.3 (1.1)	47 (2)	1.9 (0.1)
PVAc/EH-5 (melt-milled)	18	3500 (240)	41 (8)	1.2 (0.2)		
	26	3107 (522)	40 (5)	1.4 (0.2)		
PVAc/EH-5 (solution-cast)	20	2815 (89)	44 (7)	1.7 (0.3)		
	31	2739 (138)	44–52	1.8 (0.6)		

[a] The numbers in parentheses indicate the standard deviation.

perature side of the α relaxation, indicating a broadening in the distribution of relaxation times associated with the PVAc chains. Identical results were obtained for the in situ sample prepared using prehydrolyzed TEOS.

The results for two representative samples of PVAc/EH-5 prepared by solution-casting (THF) followed by melt-pressing are shown to illustrate how minor changes in sample preparation can affect the properties of the final composite. In repetitive studies, one of the samples containing a nominal 20 wt % SiO_2 exhibits a plateau in E' above T_g extending to ca. 150 °C, at which point the sample broke. Other 20 wt % samples were run and each broke before 150 °C. Curing at temperatures up to 150 °C did not improve these results. In all cases, the magnitude of E' above T_g is lower than that obtained for the in situ prepared composites and the results were not reproducible from one sample to the other. Replicate 20 wt % samples exhibited no plateau modulus above T_g and in fact started to flow. However, these samples did retain some mechanical integrity and a modulus of ca. 10^6 Pa up to about 250 °C. Similar results were obtained for PVAc composites containing ca. 20 wt % EH-5, which were cast from either a mixture of THF/EtOH (designed to simulate the final solvent conditions present in the PVAc/TEOS solution) or CCl_4. These observed differences (from sample to sample) in mechanical properties above T_g may be due to slight differences in SiO_2 content or in particle–particle connectivity or to the presence of defects resulting from sample preparation. The temperature at which the maximum in tan δ occurs is identical for all the Cab-O-Sil composites.

The results for the 30 wt % SiO_2 composites are illustrated in Figure 2. The α transition for the in situ prepared PVAc/TEOS composite is broad and the onset of T_g is shifted to a higher temperature. The magnitude of E' above T_g is higher than for the 20 wt % sample. The 30 wt % composite was cured at 150 °C for 5 h under vacuum for reasons stated above. The higher temperature required (relative to the 20 wt % composites discussed above) to remove artifacts in the temperature dependence of E' just above T_g may be due to the observed shift in T_g. All the 30 wt % EH-5 filled samples, whether prepared from solvent or melt-milled, exhibit a plateau in E' above T_g, in contrast to the 20 wt % filled samples. The melt-milled samples, however, broke repeatedly below 200 °C. In all cases, the magnitude of E' remained lower than that for the PVAc/TEOS composite, even when the SiO_2 loading in the former was higher. Identical results were obtained for EH-5 filled samples cured to 250 °C. A composite of PVAc with 30 wt % TS-720 (which is PDMS coated), prepared from THF solution, did not exhibit a plateau in E' above T_g. The PDMS surface treatment probably inhibits strong interparticle interactions by blocking

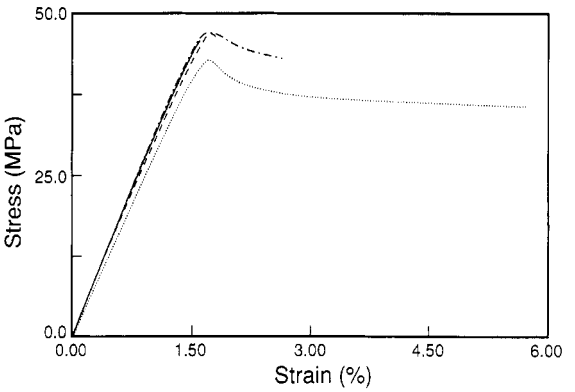

Figure 3. Stress–strain curves for in situ prepared PVAc/TEOS composites (at 26 °C) with nominal (···) 0, (– · –) 10, (– – –) 15, and (—) 30 wt % SiO_2.

surface silanols, and this prevents formation of a continuous silicate network necessary to provide the tensile strength above T_g. For all the EH-5 filled samples, the tan δ curve, and to a lesser degree the E'' curve, shows a sharp peak coinciding with the temperature of the α transition of PVAc, followed by a broad peak centered at ca. 130 °C. The origin of this second peak is not understood, but could be due to motions of PVAc chains that are restricted at the surface of the Cab-O-Sil. The loss peak for the in situ prepared sample is substantially broadened on the high-temperature side. As discussed above, the E' values in the glassy regime obtained by DMA should only be viewed as qualitative due to instrument compliance problems encountered with these thicker melt-pressed samples. More accurate values for the glassy moduli were obtained from stress–strain measurements and are reported below. Instrument compliance does not affect the measured values for the moduli in the rubbery region.

The ultimate mechanical properties, measured at ambient temperature, are summarized in Table II. The properties for both solvent-cast and melt-milled, pressed films of pure PVAc were measured to estimate reproducibility. Figure 3 shows the character of the stress–strain curves for the in situ composites of increasing silica content. The nature of the curves changes from ductile to brittle as the concentration of SiO_2 increases from 10 to 15 wt %. This also corresponds to the composition range in which a plateau in the modulus above T_g appears in the DMA analysis.[16] The addition of silica increases the modulus and decreases the elongation to break as expected. Although there is some scatter in the data, the mechanical properties below T_g are all similar, independent of the method of silica incorporation, in contrast to the DMA results obtained above T_g, where the in situ method resulted in composites with higher rubbery moduli.

Table III. Temperature Dependence of the Mechanical Properties[a]

sample	wt % SiO_2	tensile modulus (MPa) 26 °C	38 °C	49 °C	66 °C	break strain (%) 26 °C	38 °C	49 °C	66 °C
PVAc/TEOS	0	2745 (60)	239 (63)			5.2 (1.9)	456 (28)		
	7	2907 (74)	484 (38)	13 (2)		3.0 (1.0)	302 (17)	684 (10)	
	12	3059 (62)	970 (113)	55 (8)		3.0 (0.9)	243 (50)	427 (43)	
	16	3089 (213)	898 (55)	229 (33)	12 (3)	2.0 (0.3)	144 (36)	278 (26)	600 (100)
	21	3224 (295)	1156 (109)	661 (81)	91 (3)	2.0 (0.3)	84 (7)	170 (33)	340 (18)
	28	3164 (243)	2247 (313)	1832 (144)	345 (63)	1.0 (0.2)	3 (0.9)	26 (16)	40 (—)
PVAc/EH-5 (melt-milled)	18	3500 (239)		30 (4)		1.2 (0.2)		>755	
	26	3107 (522)		103 (9)		1.4 (0.2)		406 (15)	
PVAc/EH-5 (solution-cast)	20	2815 (88)		54 (8)		1.7 (0.3)		433 (50)	
	31	2739 (138)		98 (16)		2.1 (0.2)		279 (—)	

[a] The numbers in parentheses indicate the standard deviation.

Although DMA probes the mechanical response of a material subjected to extremely small deformations (the linear viscoelastic regime), the differences observed for these composites by DMA are directly reflected in their ultimate properties at temperatures even slightly above T_g. Unfortunately, temperatures corresponding to the plateau region of E' were not experimentally attainable using our equipment and thin films; however, mechanical properties of some samples were obtained at temperatures above ambient. These results are presented in Table III. Since these temperatures correspond to the glass transition regime for these composites, the modulus and break stress values are observed to decrease, whereas the strain to break increases with temperature. These effects are much less pronounced as more TEOS is added to the PVAc. Furthermore, as the SiO_2 content of the in situ prepared composites is increased, the sample properties remain measurable to higher temperatures, indicating an increase in use temperature. This is essentially a reflection of the decrease in the rate of drop in E' as a function of temperature in the glass transition regime (see the DMA results) and the slight increase in T_g as a function of increasing silicate content. Although the DMA curves for PVAc and the Cab-O-Sil filled samples look identical near the onset of T_g, the values obtained for the moduli at 49 °C for the EH-5 samples do show an increase over that of pure PVAc. This effect is much less pronounced than was observed for the in situ samples for which the onset of T_g was shifted to slightly higher temperatures.

Dielectric Relaxation. The dielectric data were taken at a series of different temperatures and normalized via time–temperature superposition. In general, the loss factor vs frequency curves for the sample containing 20 wt % EH-5, prepared by melt-blending and subsequent compression-molding, reveal two features. A single but broad relaxation peak and a slight increase in ϵ'' at high temperature and low frequency is seen (not shown) that can be attributed to dc conductivity of the sample. The master curve for this sample is shown in Figure 4 and its half-width is similar to that of pure PVAc.[16] Within experimental error and the limited attainable frequency range, the breadth of the relaxation was independent of temperature for pure PVAc and for the filled composites, and time–temperature superposition of the data was successful. While these results are consistent with those reported by Ishida for PVAc,[34] it should be noted that Sasabe and Moynihan, using a wider frequency range, have suggested that the breadth of the distribution of the relaxation times is slightly temperature dependent for PVAc.[35]

For the sample containing 20 wt % SiO_2 that was in situ polymerized and cured at 140 °C, the primary relaxation peaks are considerably broader than for either PVAc or the particle-filled samples. In addition, the half-width of the relaxation peak is slightly temperature dependent. As

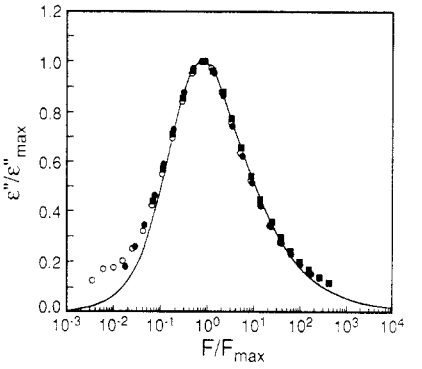

Figure 4. Normalized dielectric loss curve for the melt-milled PVAc composite containing 18 wt % EH-5. Data taken at (■) 65, (●) 69, and (○) 77 °C. The solid line represents the best fit for β to the data.

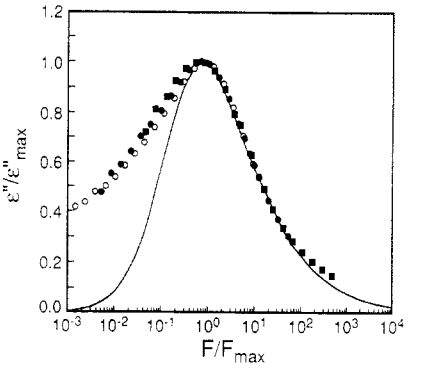

Figure 5. Normalized dielectric loss curve for the in situ prepared PVAc/TEOS composite containing 21 wt % SiO_2. Data taken at (■) 78, (●) 91, and (○) 103 °C. The solid line represents the best fit for β to the data.

seen in Figure 5, time–temperature superposition of the data was successful at higher frequencies but was marginal at the lower frequencies. In our previous work,[16] time–temperature superposition of the data for the PVAc/TEOS composites (cured at 100 °C) was less successful than is shown here. For the present work, a curing temperature of 130-140 °C was determined to be optimal (as discussed in the DMA section) to minimize further condensation of the silicate network during the measurement process. This resulted in better time–temperature superposition of the DE data. Further, since the frequency scans were made at temperatures between 80 and 117 °C (far below the curing temperature), it is suggested that the changing half-width is not due to further condensation of the TEOS. Rather, it is believed that the change in shape reflects the chemically heterogeneous environment that the polymer chains encounter.

The DE data for both in situ and Cab-O-Sil filled PVAc were analyzed in terms of the Williams–Landel–Ferry (WLF)[36] relationship, taking T_g (obtained from DSC) as

the reference temperature. The values obtained for C_1 and C_2 for PVAc were 15.5 and 56.1, respectively. Within experimental error, the values obtained for the PVAc/TEOS and PVAc/EH-5 samples (with 20 wt % SiO_2) were all very similar to those for the pure PVAc, suggesting that the fractional free volume and volume expansion of the PVAc matrix in the filled polymers are similar to those in pure PVAc. However, the shapes of the relaxation curves for in situ and Cab-O-Sil filled PVAc are indeed very different. These differences are better interpreted in terms of the Kohlrausch–Williams–Watts (KWW) function[37-39] and, alternatively, a model proposed by Schonhals and Schlosser.[40]

The distribution of relaxation mechanisms can be quantified by fitting the data to the empirical KWW function.[37-39] The form of the relaxation function is given by the fractional exponential

$$\phi(t) = e^{-(t/\tau)^{\beta}} \quad (1)$$

where β is the distribution parameter ($0 < \beta \leq 1$). This parameter characterizes the breadth of the relaxation time spectrum for the PVAc chains.[41]

Analysis of the data for the composite of PVAc and 20 wt % EH-5 prepared by melt-milling (Figure 4) indicates that the best fit to the data is obtained for a value of β equal to 0.58. A similar value of β has previously been reported for pure PVAc,[16] suggesting that the larger, preformed particles do not influence the distribution of relaxation times in the vicinity of the glass transition. Identical values of β (0.58 ± 0.02) were obtained for the other composites containing 20 wt % filler, independent of the method of sample preparation and filler type.

As previously reported for samples prepared by in situ polymerization, there is a corresponding increase in the distribution of relaxation times with increasing concentration of SiO_2.[16] Further analysis of the sample containing 20 wt % SiO_2 cured at 140 °C (shown in Figure 5) is revealing. While it is clear that this master curve is considerably broader than for the sample shown in Figure 4, most of the broadening occurs on the low-frequency side. The low-frequency broadening is not believed to be the result of dc conductivity, since a similar type of broadening is observed on the high-temperature side of the α relaxation in the DMA spectrum. It was not possible to fit the entire data set to the KWW function. Therefore, the best fit value of β was calculated by fitting the data only at high frequency. The value of β decreased to approximately 0.49 due to the influence of the SiO_2 network.

For the melt-milled sample containing 30 wt % EH-5, thought to be a better comparison with the in situ composites since it exhibited a plateau in E' above T_g, the value of β is seen to decrease slightly to 0.55. A slight broadening at the low-frequency end (shown in Figure 6) is also observed. These results suggest that at this higher concentration, the particles may have begun to influence the breadth of the relaxation time distribution. In contrast to the DMA results, two distinct relaxation peaks were not observed in the dielectric data.

In a recent paper by Schonhals and Schlosser, a model was proposed to describe the shape of the dielectric relaxation curve.[40] The authors suggest that the models that describe the relaxation curve with a single parameter may not provide an adequate description of the relaxation process. While it is not the purpose of this paper to distinguish between the merits of each of the models, it is perhaps true that the two-parameter model may provide additional information that can help interpret the underlying mechanism for the broadening at the glass transition for the in situ polymerized composites.

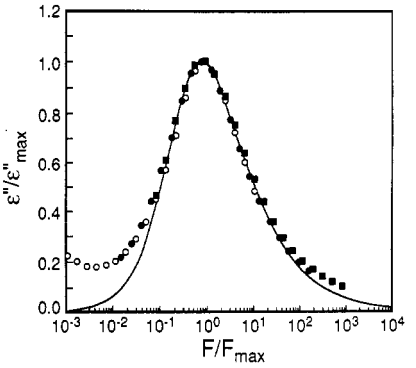

Figure 6. Normalized dielectric loss curve for the melt-milled PVAc composite containing 27 wt % EH-5. Data taken at (■) 68, (●) 77, and (○) 93 °C. The solid line represents the best fit for β to the data.

The main feature of the model is that two parameters, m and n, can describe the frequency dependence of the loss factor separately. In the limit of low and high frequency, the loss factor is then given by the scaling relations shown in the equations

$$\epsilon''(\omega) \sim \omega^{m} \quad (\omega \ll \omega_0) \quad (2)$$

and

$$\epsilon''(\omega) \sim \omega^{-n} \quad (\omega \gg \omega_0) \quad (3)$$

In these equations ω is the angular frequency, ω_0 is the maximum in the frequency scale at a given temperature, and m and n are parameters used to characterize the shape of the relaxation curve. In the limit of extremely dilute solutions, model functions have been shown to increase with $\sim\omega^{m}$ ($m = 1$) at low frequency and decay with $\sim\omega^{-n}$ ($0.5 \sim n < 1$) at high frequency. The authors suggested that the mechanism of local dynamics would not change in solid polymers compared to dilute solutions. However, the diffusional propagation of orientation along the chain would be dampened and a value of $n < 0.5$ would be anticipated. Further, values of $m < 1$ would be expected and would decrease with increasing large-scale correlations. Therefore, it is suggested that the parameter n can describe the dielectric loss at high frequencies and is related to the local chain dynamics, and m is related to the longer range and interchain cooperative motions. The parameter m has been observed to decrease with increasing large-scale correlation such as crystallinity, cross-linking, and hydrogen bonding.[40]

The values of m and n were calculated for PVAc and the in situ polymerized composite containing 20 wt % SiO_2. Due to the limited frequency range available for the dielectric experiments, it was necessary to analyze the data at various temperatures to obtain enough data in both the high- and low-frequency limits. The results, shown in Table IV, indicate that the values of n are less than 0.5 and values of m are less than 1.0, as predicted by the model. Comparing PVAc to the sample containing 20 wt % SiO_2 indicates that the differences in the value of n are small compared to changes in m. The results suggest that while the SiO_2 network certainly influences, and presumably hinders, motions of the PVAc chains, it is the longer range motions that are the most significantly restricted. To appreciate the degree to which long-range motions are restricted, it should be noted that the value of m at the glass transition for the in situ polymerized composite is smaller than for both a cross-linked epoxy (m varies between 0.24 and 0.51 depending on the curing agent) and

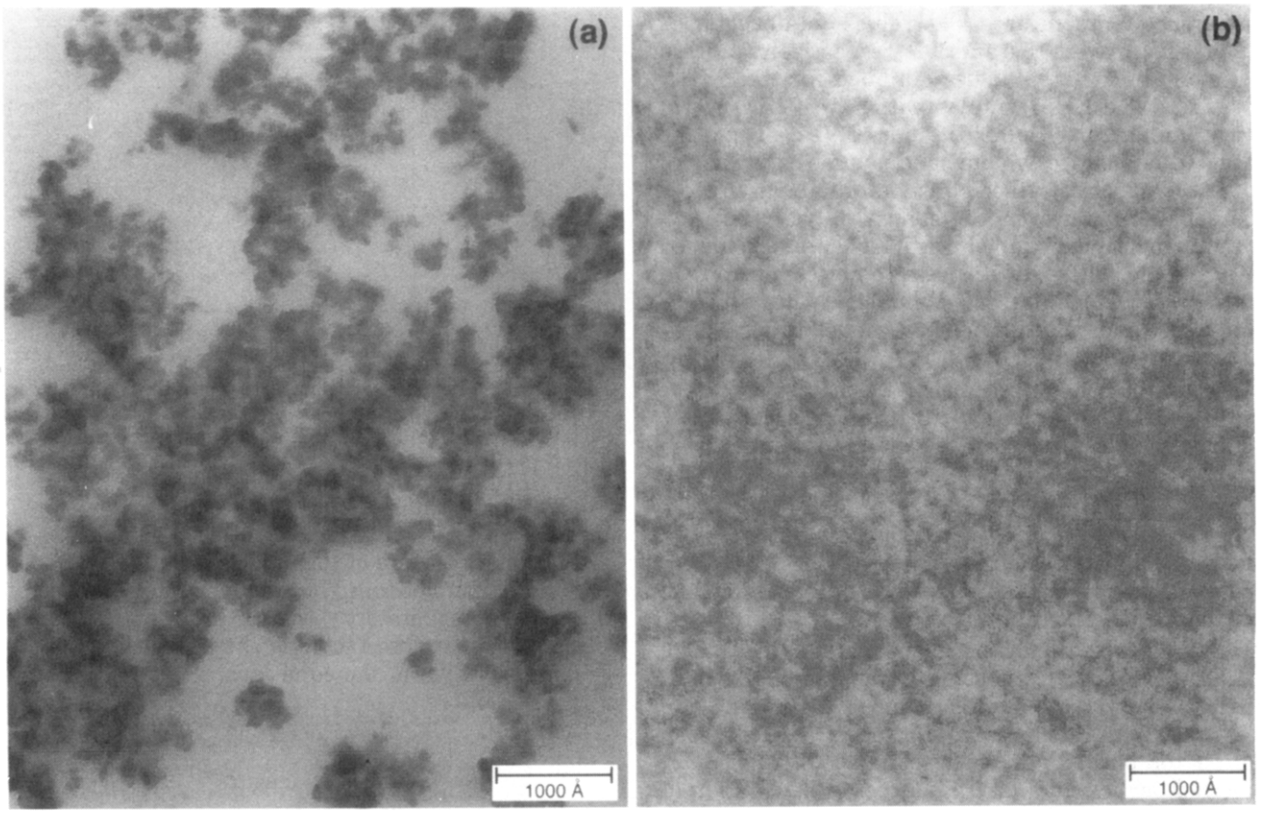

Figure 7. Transmission electron micrographs for (a) the PVAc composite with 20 wt % EH-5 cast from THF and (b) the in situ prepared PVAc/TEOS with 16 wt % SiO_2.

Table IV. Shape Parameters *m* and *n* at Various Temperatures for PVAc and the Composites

sample	T (°C)	n	m
PVAc	68.5	0.390	
	93.0		0.691
PVAc/TEOS (20%)	74.0	0.347	
	84.0	0.363	
	102.0		0.146
	110.0		0.162
PVAc/EH-5 (20%, melt-milled)	68.0	0.401	
	92.5		0.546
PVAc/EH-5 (30%, melt-milled)	68.0	0.381	
	92.5		0.450

for a crystalline sample of poly(ethylene terephthalate) (PET) (m decreased from 0.81 for amorphous PET to 0.36 for crystallized PET).[40] Also shown in Table IV are the values of m and n obtained for the melt-milled composites containing 20 and 30 wt % EH-5. The results show that with increasing concentration of EH-5 there is a decrease in the value of m while n remains essentially constant. The addition of the particle appears to influence primarily the longer range motions of the polymer chains. However, the degree to which the motions are restricted, even at 30 wt % filler are far less than the restrictions encountered for the sample containing 20 wt % SiO_2 that was prepared from the in situ polymerization of TEOS. The present analysis highlights the larger differences between the shapes of the dielectric relaxation curves obtained for in situ vs particle-filled composites to a greater extent than did the KWW analysis. This model is better able to fit the wings of the distribution while the KWW function is typically optimized around the half width of the curve.

Morphology. Transmission electron micrographs for the PVAc/EH-5 (20 wt %) composite cast from THF and the PVAc/TEOS composite (15 wt % silica) are shown in Figure 7. Each reveals that despite the optical transparency of the composite films, a microscopic heterogeneity exists. Qualitative differences are apparent between the two morphologies with respect to the primary (smallest) particle size, the size of phase heterogeneity, and the sharpness of the polymer/filler interface. In the Cab-O-Sil system, aggregates of the filler particles are clearly visible, and within the resolution of the micorgraph, particle–matrix boundaries are visible. Similar morphologies are observed by TEM for the melt-milled PVAc/EH-5 (20 wt %) and solution-cast PVAc/EH-5 (30 wt %) samples. Lower magnification images (not shown here) also indicate that the aggregates are evenly dispersed by the melt-milling and solution-casting procedures. The absence of large, i.e., micron-sized, clusters is supported by the fact that the films are optically transparent. The inhomogeneity of the two phases, reflected by the "pockets" of the lighter shade polymer, is a manifestation of the random nature of individual clusters and their inherent packing inefficiency.

The micrograph of the PVAc/TEOS system (Figure 7b) seems to indicate a two-phase morphology, but of a much finer texture than in the Cab-O-Sil filled materials. Moreover, the boundary between the inorganic and organic phases is indistinct even at the highest magnification, indicating a more intimate mixture of the two phases. Composition fluctuations between the lighter organic phase and the darker inorganic structure continue to exist. Although one should be cautious when interpreting a two-dimensional image of a three-dimensional structure, particularly with the finite depth of field (ca. 50 nm) which is much greater than the size of the compositional heterogeneity, it appears that the inorganic network phase is evenly distributed throughout the composite.

Several of the PVAc/Cab-O-Sil and PVAc/TEOS composites were examined by SAXS to probe the local structure of the inorganic phase at distance scales of approximately 100 nm and smaller. The SAXS profiles for PVAc/Cab-O-Sil mixtures are reported first. De-

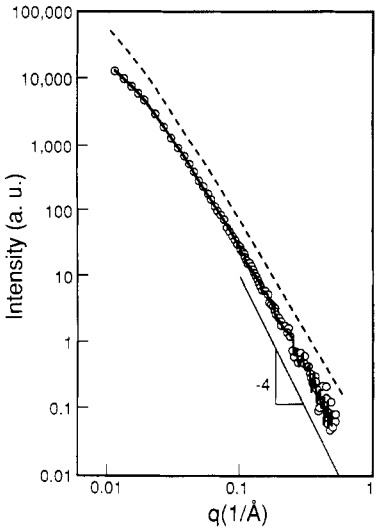

Figure 8. SAXS profiles of PVAc composites containing 20 wt % EH-5 prepared by (○) solution (THF) casting and (—) melt-milling. The limiting power law slope of −4 indicates a smooth interface exists between the PVAc and the silica filler. The dashed line, shifted for clarity, represents data taken by Hurd et al.[42] on a dilute solution of EH-5.

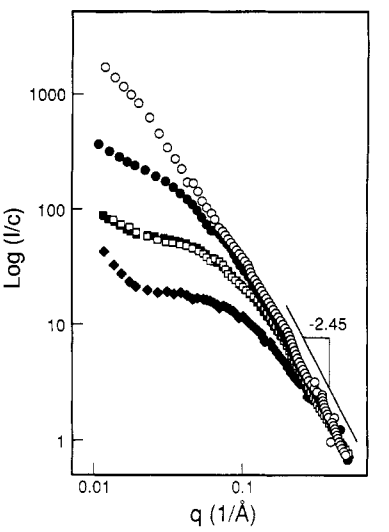

Figure 9. SAXS profiles for in situ prepared PVAc/TEOS with nominal (○) 5, (●) 10, (□) 15, (■) 20, and (♦) 30 wt % SiO_2.

smeared scattering curves of intensity vs scattering vector q for two of the composites containing 20 wt % EH-5 prepared by melt-milling and solution-casting methods are given in Figure 8 in the form of a log–log plot. The two data sets superpose exactly upon normalization according to slight volume fraction differences. Identical scattering profiles are observed for the samples with 30 wt % loading of EH-5 as well as for those containing MS-7 and TS-720. It also appears that, within the resolution of the SAXS experiment, the local structure of the silica aggregates is the same whether the composites were prepared by solution casting and pressing or by melt-milling.

Information about the interface in the PVAc/Cab-O-Sil system is obtained from the limiting power law behavior in the Porod region. The final power law slope of −4 at the highest q's indicates that the surface of the primary silica particles is smooth and that a sharp interface exists between the organic and inorganic phases.[42] Hurd et al.[43] have suggested that certain Cab-O-Sils, including EH-5, may have fractally rough surfaces. Within the resolution of our SAXS data, we cannot distinguish whether the same is observed here. In any event, the question of fractally rough surfaces vs smooth surfaces of the filler particles is beyond the scope of this study.

At intermediate scattering angles, starting at length scales of approximately 5 nm and up, the profiles demonstrate the fractal nature of the silica aggregates of Cab-O-Sil. To reiterate the observation that the Cab-O-Sil structure is not substantially changed upon dispersal in PVAc, the results of Hurd et al.[43] of small angle neutron and light scattering measurements on dilute aqueous dispersions of Cab-O-Sil EH-5 are reproduced in Figure 8 by the dashed line. This scattering curve was calculated from parameters determined by an empirical fit,[43] and has been shifted slightly along the intensity axis for clarity. A slight difference exists between Hurd and co-workers and our data at the low q values for the SAXS data. This difference may persist to larger length scales accessible by light scattering. It is clear that the local structure of the silica aggregates is quite similar, with perhaps some differences at larger scales. Overall, it appears that the inorganic clusters retain their fractal character, which probably contributes to the packing inefficiency seen in the electron micrographs. Since the scattering profiles for all the Cab-O-Sil composites are the same, it appears that the SAXS experiment is unable to resolve differences in connectivity of aggregates that lead to the onset of a plateau in E' above T_g. This is because the Cab-O-Sil aggregates themselves have been shown[43] to already be of 100–200 nm in size, just beyond the resolution for SAXS.

The desmeared SAXS profiles for five compositions of the in situ prepared PVAc/TEOS composites, normalized for volume fraction of the inorganic phase, are reported in Figure 9 in the form of a log–log plot. Each profile approaches a limiting slope of −2.45, indicating that the structures are mass fractals. The superposition of all the profiles at high q indicates that the inorganic phase for each sample on length scales smaller than about 5–7 nm are identical. The inorganic matrix continues to exhibit mass fractal behavior out to high q, that is, down to ca. 1–2 nm lengths. Since the combination of PVAc and silicate network phases must be space-filling, this suggests that the PVAc is intimately mixed with the inorganic network. Intimate mixing may lead to chain entrapment, a notion proposed earlier.[16] Additionally, the polymer is exposed to a much larger inorganic "surface" area and has access to pendant OH groups on the silicate skeleton for hydrogen bonding.

At intermediate scattering vectors, the power law slope for the 5 wt % (TEOS) sample changes to approximately −2.0. This may reflect a slight change in the silicate network growth at larger distances, as well as the manifestation of cluster polydispersity.[44] For the higher TEOS loadings, particularly from 15 to 30 wt % SiO_2, the profiles level off. This is believed to be caused by the overlap and interpenetration of distinct clusters of silica. Such overlap of distinct clusters would screen the range over which fractal correlations exist within a cluster. Screening effects have been proposed for systems where TEOS is polymerized in solution.[45] The onset of the silicate cluster overlap, and subsequent interreactions, may be what provides connectivity and support of these materials beyond T_g.

Infrared Results. The presence of extensive hydrogen bonding between residual silanols on the silicate network and the carbonyl of PVAc is characteristic of in situ prepared composites and has been reported previously.[16] Both MS-7 and EH-5 Cab-O-Sil particles have available free hydroxyl (OH) groups that can participate in hydrogen bond formation. Hydrogen bonding between silica fillers

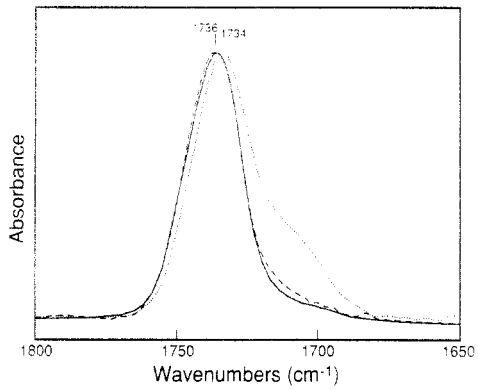

Figure 10. FTIR-ATR spectra of the carbonyl region for (···) PVAc/TEOS, (– – –) PVAc/EH-5 cast from THF, and (—) PVAc/EH-5 melt-milled. All composites have nominally 30 wt % SiO_2.

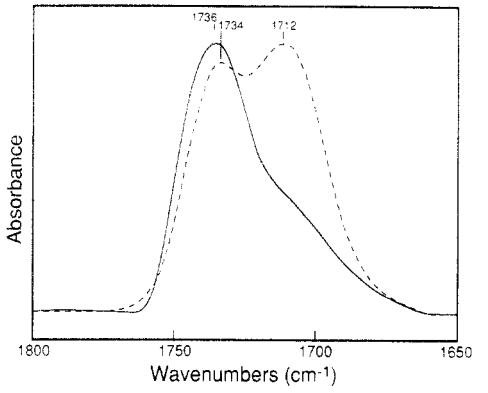

Figure 11. Transmission FTIR spectra for (– – –) PVAc/TEOS and (—) partially dried PVAc/EH-5 in THF. Both composites have nominally 50 wt % SiO_2.

and PVAc *in solution* is well documented.[46] ATR spectroscopy was used to obtain the spectra directly on the films. However, as shown in Figure 10, no indication of hydrogen bonding is evident between the EH-5 and PVAc in the dried film composites with 30 wt % SiO_2. Similar results were obtained for the PVAc/MS-7 composite. In contrast, the in situ prepared film exhibits substantial hydrogen bonding, as evidenced by the shift to lower wavenumbers of a portion of the carbonyl stretching band. The presence of hydrogen-bound carbonyl groups in mixtures of PVAc and EH-5 is indeed observed when the concentration of SiO_2 is increased to 50 wt % and solutions of the mixture are cast from THF or CCl_4 directly between two KBr disks. This is shown in Figure 11. As the sample dries, the carbonyl peak splits into a free and a bound peak, the latter of which grows with time. However, during the drying process the sample becomes white and powdery at such high loadings of SiO_2. This introduces some contributions due to scattering and/or optical dispersion, which increase the background signal and broaden and shift the carbonyl peak. The relative lack of hydrogen bonding between PVAc and Cab-O-Sil was surprising in light of previous studies indicating strong interactions, at least in solvents such as CCl_4.[46] Since THF could compete with PVAc for the surface of the silica particles (and thereby displace PVAc), samples were also cast from CCl_4. These results were indistinguishable from the THF results. The results for a composite containing 50 wt % EH-5 are compared to those of an in situ prepared sample of the same composition in Figure 11. Although interactions are observed for both samples, the amount of hydrogen-bound carbonyls is substantially greater for the latter. This is reasonable since there will be less free OH groups on the EH-5 (as they are restricted to the surface of the dense particles) than in the more ramified silicone network formed from acid-catalyzed TEOS. It is also consistent with the notion of less intimate mixing of the organic and inorganic (EH-5) phase, as discussed in the morphology section.

Finally, when comparing the Cab-O-Sil vs TEOS composites, one may question whether the large amount of hydrogen bonding observed in PVAc/TEOS could be due to water or ethanol from the in situ reaction. Thus, mixed solvents of THF/EtOH (adding 4 equiv of ethanol per mole of Si to emulate the TEOS reactions), as well as THF/EtOH with 2 equiv of 0.15 M HCl, were used to prepare the PVAc/EH-5 composites. In no case could substantial hydrogen bonding be detected with the Cab-O-Sil particles.

Discussion

This study was designed to identify differences in composites generated from PVAc with either fumed silica particles or in situ polymerized (under acidic conditions) TEOS at relatively low loadings (<40 wt%) of silica. The smallest commercially available particle size for the fumed silica was chosen to compare with the size of the silicate particles produced in situ. However, these were still much larger than what is believed to be the primary particle size produced from the acid catalyzed in situ polymerization of TEOS.

The combined results, high plateau modulus above T_g, broadened distribution of relaxation times at T_g, diffuse interface between silica and PVAc, and a high level of hydrogen bonding, suggest that the in situ composites are composed of interpenetrating PVAc chains and silicate network. The PVAc chains are strongly adsorbed to, and entrapped in, the silicate network.[16] The observation that identical DMA results are obtained when prehydrolyzed TEOS (where presumably formation of the primary silica particle has already occurred) is added to the PVAc solution immediately prior to casting suggests that the enhanced physical properties are not a result of interpenetration of PVAc chains within the primary particles of the growing silicate network. The interpenetration of PVAc and silicate occurs on a different level. The improved mechanical properties are proposed to be due to the presence of a "percolated" SiO_2 network, which is predominantly responsible for the mechanical integrity of the sample above the T_g of PVAc. Presumably, this network results from continued condensation of inorganic oligomers during drying and curing. The idea of a continuous network of silica particles is consistent with that proposed by Mauritz[22] for Nafion/TEOS composites. Although the possibility of cross-linking occurring between PVAc and the silicate exists, it is not believed that this would account for the experimental observations discussed herein.

Identical networks do not appear to be generated using the particle-filled approached. These composites show much sharper interfaces between the organic and inorganic phases, and the polymer relaxations are not altered to a large degree by the presence of the silicate. Although a continuous silicate network can apparently be formed via the fumed silica particles, as indicated by the plateau modulus, much higher loadings of SiO_2 are required to reach this threshold than in the in situ approach. This may be due to differences in sizes of the primary particles and to the fact that it is difficult to completely disrupt the preformed Cab-O-Sil aggregates, even during melt-milling.

These differences may also be due in part to the differences in sample preparation. Whereas melt-milling

should, in principle, be capable of disrupting the fumed silica aggregates, these particles may not be able to reorganize into a continuous network as the composite is quenched. The in situ samples are solution-cast, which provides time for diffusion of silicate oligomers. These would have high mobility (relative to particles) and can migrate and further react to generate a continuous network. Solution-cast, particle-filled samples do have the necessary mobility for diffusion to take place; however, these were far more heterogeneous than castings of the in situ samples. A low volume percent of micron-size voids was observed by TEM in the solvent-cast PVAc/EH-5 composites. These were not successfully eliminated by repeatedly treating the samples to high-temperature vacuum conditions, followed by high-temperature melt-pressing conditions. These voids were not observed in the in situ nor the melt-milled composites. The presence of these voids would result in an apparent lower modulus (the estimated error would be less than 10%) measured by DMA. These will also act as stress-concentration points (defects) and may explain the slightly lower results obtained in the stress–strain experiments for the solvent-cast vs melt-milled PVAc/EH-5 composites. However, the presence of these voids does not influence the conclusions concerning the morphology and interface between the silicate and PVAc derived from SAXS and TEM experiments.

Phase separation is also retarded during the sample preparation via strong interactions (H-bonding) between the silicate and the polymer. The ramified network structures produced in situ would have relatively large numbers of silanols with which to interact with the polymer. The fumed silica particles have much less surface area and less surface silanols. The number of silanols available for hydrogen bonding undoubtedly retards phase separation and helps dictate the network formation.

Conclusions

Transparent composite samples were readily produced via the in situ method or by melt-blending fumed silica. However, the melt-blending procedure does not lend itself to coatings applications. Solution-coating or -casting techniques using the fumed silica resulted in opaque, inhomogeneous samples. With either approach, the fumed silica composites required a final hot-pressing step.

Dielectric studies of the loss peak at T_g showed that composites made from any of the fumed silica particles had β values similar to that obtained for pure PVAc. However, the in situ composites had substantially smaller values of β, indicative of a broader distribution of relaxation times for the PVAc chains. These latter composites also showed substantial broadening in the low-frequency region, consistent with the observed broadening of the high-temperature side of α peak for the in situ composites by DMA. The asymmetric nature of the DE data for the in situ composites was better fit to a two-parameter model by Schonhals and Schlosser,[40] suggesting that the silicate network greatly influences large-scale dynamic correlation of the PVAc polymer chains.

TEM and SAXS studies indicated that microscopic heterogeneity exists in both the particle-filled and in situ composites, although the latter composites appeared to be more intimately mixed. Presumably neither melt-milling nor solution-casting completely disrupts the aggregates present in the fumed silica. Additionally, the particle-filled materials were shown to have much sharper interfaces between the organic and inorganic phases than did the in situ composites, consistent with more intimate mixing of the phases by growing the silicate network in situ.

Infrared results indicated that the in situ composites exhibit substantial hydrogen bonding between the carbonyl oxygens of PVAc and silanols of the silicate network. Little or no hydrogen bonding was detectable in the particle-filled composites. These differences are likely due to both the substantially smaller number of available surface silanols on the fumed silica particles and a less intimate mixing between the polymer and the inorganic phases and are a reflection of the large differences in silicate surface areas.

Little or no difference in ultimate mechanical properties was observed in the glassy state for the particle-filled or in situ composites. However, substantial differences were obtained above the T_g of PVAc. Increasing the amount of added SiO_2 via polymerization of TEOS resulted in small increases in polymer T_g, whereas no increase in T_g was observed by addition of fumed silica. A rubberlike plateau in the tensile storage modulus above T_g, which extended to nearly 300 °C, was observed via the in situ approach at SiO_2 loadings of 15 wt % or higher. At this composition, the stress–strain curves reflected a change from ductile-to-brittle failure behavior for the composites. The value of this modulus increased with increasing SiO_2 content. On the other hand, it was difficult to obtain reproducible samples with the particle-filled composites which would exhibit a plateau in the moduli above T_g for loadings less than 30% SiO_2. In all cases the value of the plateau modulus for the particle-filled composites was lower than that for the in situ materials having the same loading of SiO_2. Although little difference was observed in the mechanical properties of particle-filled and in situ composites below T_g, the in situ approach led to materials with improved high-temperature properties.

Thus, it is proposed that continuous silicate networks form in both types of composites and, once formed, these networks dominate the mechanical properties at elevated temperatures. However, these networks form at lower loadings and are much more intimately mixed with the organic polymer when produced via in situ polymerization of TEOS.

Acknowledgment. We thank Wilson Yetter for the electron microscopy. We are also grateful for the technical assistance of Tonya Binga and Erika Abbas.

References and Notes

(1) Plueddemann, E. P. *Silane Coupling Agents*; Plenum Press: New York, 1982.
(2) Arkles, B. *CHEMTECH* **1977**, *7*, 766.
(3) Mark, J. E. *Br. Polym. J.* **1985**, *17*, 144.
(4) Sur, G. S.; Mark, J. E. *Eur. Polym. J.* **1985**, *21*, 1051.
(5) Clarson, S. J.; Mark, J. E. *Polym. Commun.* **1987**, *28*, 249.
(6) Sun, C.-C.; Mark, J. E. *Polymer* **1989**, *30*, 104.
(7) Huang, H. H.; Orler, B.; Wilkes, G. L. *Macromolecules* **1987**, *20*, 1322.
(8) Brennan, A. B.; Rabbani, F. *Polym. Prepr. (Am. Chem. Soc., Div. Polym. Chem.)* **1991**, *32* (3), 496.
(9) Glaser, R. H.; Wilkes, G. L. *J. Non-Cryst. Solids* **1989**, *113*, 73.
(10) Noell, J. L. W.; Wilkes, G. L.; Mohanty, D. K.; McGrath, J. E. *J. Appl. Polym. Sci.* **1990**, *40*, 1177.
(11) Coltrain, B. K.; O'Reilly, J. M.; Turner, S. R.; Sedita, J. S.; Smith, V. K.; Rakes, G. A.; Landry, M. R. In *Proceedings of Fifth Annual International Conference on Crosslinked Polymers*, Switzerland, 1991, p 11.
(12) Coltrain, B. K.; Rakes, G. A.; Smith, V. K. US Patent 5,019,607, 1991.
(13) Schmidt, H. *J. Non-Cryst. Solids* **1989**, *112*, 419.
(14) Pope, E. J. A.; Asami, M.; Mackenzie, J. D. *J. Mater. Res.* **1989**, *4*, 1018.
(15) Klein, L. C.; Abramoff, B. *Polym. Prepr. (Am. Chem. Soc., Div. Polym. Chem.)* **1991**, *32* (3), 519.
(16) (a) Fitzgerald, J. J.; Landry, C. J. T.; Schillace, R. V.; Pochan, J. M. *Polym. Prepr. (Am. Chem. Soc., Div. Polym. Chem.)* **1991**,

32 (3), 532. (b) Fitzgerald, J. J.; Landry, C. J. T.; Pochan, J. M. *Macromolecules* **1992**, *25* (14), 3715.
(17) Landry, C. J. T.; Coltrain, B. K.; Brady, B. K. *Polymer* **1992**, *33* (7), 1486.
(18) Landry, C. J. T.; Coltrain, B. K.; Wesson, J. A.; Zumbulyadis, N.; Lippert, J. L. *Polymer* **1992**, *33* (7), 1496.
(19) Coltrain, B. K.; Ferrar, W. T.; Landry, C. J. T. US Patent 5,010,128, 1991.
(20) Coltrain, B. K.; Ferrar, W. T.; Landry, C. J. T.; Molaire, T. R.; Zumbulyadis, N. *Chem. Mater.* **1992**, *4*, 358.
(21) Mauritz, K. A.; Warren, R. M. *Macromolecules* **1989**, *22*, 1730.
(22) Mauritz, K. A.; Storey, R. F.; Jones, C. K. *ACS Symp. Ser.* **1989**, *395*, 401.
(23) Mauritz, K. A.; Jones, C. K. *J. Appl. Polym. Sci.* **1990**, *40*, 1401.
(24) David, I. A.; Scherer, G. W. *Polym. Prepr. (Am. Chem. Soc., Div. Polym. Chem.)* **1991**, *32* (3), 530.
(25) Wung, C. J.; Pang, Y.; Prasad, P. N.; Karasz, F. E. *Polymer* **1991**, *32*, 605.
(26) Ellsworth, M. W.; Novak, B. M. *J. Am. Chem. Soc.* **1991**, *113*, 2756.
(27) Novak, B. M.; Davies, C. *Macromolecules* **1991**, *24*, 5481.
(28) Ellsworth, M. W.; Novak, B. M. *Polym. Prepr. (Am. Chem. Soc., Div. Polym. Chem.)* **1992**, *33* (1), 1088.
(29) Brinker, C. J. *J. Non-Cryst. Solids* **1988**, *100*, 31.
(30) Iler, R. K. *The Chemistry of Silica*; John Wiley & Sons: New York, 1979.
(31) Craievich, A.; Aegerter, M. A.; dos Santos, D. I.; Woignier, T.; Zarzycki, J. *J. Non-Cryst. Solids* **1986**, *86*, 394. A skeletal density of 2.2 g cm^{-1} is reported for silica aerogels prepared under neutral conditions, as opposed to the acidic conditions employed for our samples. This value gave the best results when calculating the silicate phase volume fraction with respect to the SAXS profile behavior in the Porod region.
(32) Glatter, O. *J. Appl. Crystallogr.* **1974**, *7*, 147.
(33) Brinker, C. J.; Scherer, G. W. *Sol–Gel Science: The Physics and Chemistry of Sol–Gel Processing*; Academic Press: Boston, 1990; pp 537–538.
(34) Ishida, Y.; Matsuo, M.; Yamafugi, K. *Kolloid Z. Z. Polym.* **1961**, *180*, 108.
(35) Sasabe, H.; Moynihan, C. T. *J. Polym. Sci., Polym. Phys. Ed.* **1978**, *16*, 1447.
(36) Ferry, J. D. *Viscoelastic Properties of Polymers*; John Wiley: New York, 1980.
(37) Williams, G.; Watts, D. C. *Trans. Faraday Soc.* **1970**, *66*, 2503.
(38) Williams, G.; Watts, D. C.; Dev, S. B.; North, A. M. *Trans. Faraday Soc.* **1971**, *67*, 1323.
(39) Kohlrausch, R. *Ann. Phys.* **1847**, *12* (3), 3931.
(40) Schonhals, A.; Schlosser, E. *Colloid Polym. Sci.* **1989**, *267*, 125.
(41) Moynihan, C. T.; Boesch, L. P.; Laberge, N. L. *Phys. Chem. Glasses* **1973**, *14* (6), 122.
(42) Porod, G. *Kolloid Z.* **1951**, *124*, 83.
(43) Hurd, A. J.; Schaefer, D. W.; Martin, J. E. *Phys. Rev. A* **1987**, *35*, 2361.
(44) Martin, J. E.; Hurd, A. J. *J. Appl. Crystallogr.* **1987**, *20*, 61.
(45) Cabane, B.; Dubois, M.; Duplessix, R. *J. Phys. (Paris)* **1987**, *48*, 2131.
(46) (a) Thies, C. *Macromolecules* **1968**, *1*, 335. (b) Koral, J.; Ullman, R.; Eirich, F. R. *J. Phys. Chem.* **1958**, *62*, 541. (c) Botham, R.; Thies, C. *J. Polym. Sci., Part C* **1970**, *30*, 369.